RESEARCH PAPER

Neurologia i Neurochirurgia Polska
Polish Journal of Neurology and Neurosurgery
2022, Volume 56, no. 5, pages: 410–416
DOI: 10.5603/PJNNS.a2022.0053

ISSN: 0028-3843, e-ISSN: 1897-4260

Unruptured intracranial aneurysms: relation between morphology and wall strength

Leszek Lombarski[1], Przemysław Kunert[1], Sylwia Tarka[2], Adam Piechna[3], Sławomir Kujawski[4], Andrzej Marchel[1]

[1]Department of Neurosurgery, Medical University of Warsaw, Warsaw, Poland
[2]Department of Forensic Medicine, Medical University of Warsaw, Warsaw, Poland
[3]Institute of Automatic Control and Robotics, Warsaw University of Technology, Warsaw, Poland
[4]Department of Exercise Physiology and Functional Anatomy, Collegium Medicum in Bydgoszcz, Nicolaus Copernicus University in Torun, Bydgoszcz, Poland

ABSTRACT

Aim of the study. To determine the morphological features distinguishing small unruptured saccular intracranial aneurysms (sIAs) with high and low wall strength (WS) in post mortem subjects.

Clinical rationale for the study: Subarachnoid haemorrhage caused by sIA rupture is associated with increased mortality and morbidity. Analysis of the morphology and biomechanical properties of sIAs might facilitate the identification of clinically relevant risk factors for sIA rupture.

Material and methods. Eight single unruptured sIAs were found among eight subjects during 184 post mortem examinations. After assessment of the dimensions, aspect ratio (AR), size ratio (SR), height/width ratio (HW), bottleneck factor (BNF), and shape, sIAs with adjacent cerebral arteries were subjected to quasi-static increasing pressure until the wall of the cerebral artery or sIA ruptured.

Results. In three specimens, the sIA ruptured at a significantly lower average pressure than the other cases, in which the rupture occurred within the wall of the adjacent cerebral artery (769 *vs.* 1,259 mmHg; $p = 0.035$). The sIAs with low WS, i.e. sIAs that ruptured during experiments, were characterised by significantly increased dome dimensions compared to sIAs with high WS ($p < 0.05$). At the same time, no significant differences were observed between high and low WS categories regarding AR, SR, HW, and BNF, or the presence of an irregular dome shape.

Conclusions and clinical implications. Dome dimension was the only feature that distinguished unruptured sIAs as having low or high WS, and this supports observations that sIAs with increased dome dimensions are characterised by an increased risk of rupture. Thus, dome dimension may be more useful than other morphometric parameters, such as AR, SR, HW and BNF, in assessing the rupture risk assessment of small unruptured sIAs.

Key words: intracranial aneurysm, aneurysm morphology, rupture risk, rupture pressure, wall strength

(*Neurol Neurochir Pol 2022; 56 (5): 410–416*)

Introduction

A saccular intracranial aneurysm (sIA) may be defined as local dilation of the cerebral artery lumen caused by weakening of the arterial wall. The risk factors for sIA rupture, which is a leading cause of non-traumatic subarachnoid haemorrhage (SAH), include smoking and hypertension, as well as morphological features of sIAs such as size ≥ 7 mm [1, 2]. Based on the results of multicentre studies, the annual rupture rate of sIAs < 5 mm is up to 0.36% [2, 3]. On the other hand, retrospective

Address for correspondence: Przemysław Kunert, Department of Neurosurgery, Medical University of Warsaw, 1a Banacha St, 02–097 Warsaw, Poland; e-mail: przemyslaw.kunert@wum.edu.pl

Received: 11.04.2022 Accepted: 24.06.2022 Early publication date: 26.07.2022

analyses have shown that 35–47% of ruptured sIAs are < 5 mm [4, 5]. Due to large discrepancies in the literature regarding sIA threshold size for rupture risk assessment, other morphometric parameters, including aspect ratio (AR), size ratio (SR), bottleneck factor (BNF), and height/width ratio (HW), have been proposed. Nevertheless, the vast majority of data comes from cross-sectional studies comparing the morphology of ruptured to that of unruptured sIAs [6, 7]. Since sIAs tend to change shape and increase the size of their dome after rupture [8], threshold values of morphometric parameters for rupture prediction may have been overestimated. Thus, such parameters may not be adequate for the stratification of SAH risk associated with an unruptured sIA [9].

Clinical rationale for the study

Irrespective of the relatively low annual risk of sIA rupture of 1.6% [10], SAH is a serious cerebrovascular event leading to death in approximately one third of cases, and severe disability in another third [2]. Unfortunately, the available preventive invasive procedures are associated with 1-year combined mortality and morbidity estimated at 10.1% and 6% for surgical treatment and endovascular treatment, respectively [11]. Hence, it is important to identify which sIAs are at greater risk of rupture and require neurosurgical treatment. Recent studies on sIA biomechanical properties have revealed differences in mechanical response during uniaxial extension tests between ruptured and unruptured sIAs, as well as between unruptured sIAs with low and high wall strengths (WS). Nevertheless, these biomechanical studies refer exclusively to a fragment of the wall of an sIA collected during surgical procedures, and do not consider the complexity of sIA wall structure [12, 13]. Therefore, studies concerning the morphology and biomechanical properties of intact, unruptured sIAs may better elucidate the clinical relevance of morphological rupture risk factors.

Material and methods

SIA specimens

From September 2016 to June 2018, we analysed brains collected during 184 consecutive forensic post mortem examinations of patients from Poland's Masovian Voivodeship with extracerebral causes of death (age 60 ± 8 years; 53 females). Cadavers were stored at 4°C before the post mortem, and the interval between death and our analysis did not exceed 36 hours. A total of eight single unruptured sIAs were identified in eight brains (age 62 ± 4 years; two females). Following a stepwise dissection of the subarachnoid cisterns, sIAs with adjacent cerebral arteries were excised using a surgical microscope (Carl Zeiss OPMI pico S100, Germany) (Fig. 1A). All experiments were performed in accordance with relevant guidelines and regulations. The approval of the local ethics committee and informed consent from family members were not required for the use of post mortem material in the present study.

Morphometric analysis

All specimens were rinsed with 0.9% NaCl solution to remove blood clots. The specimens were then subjected to pressure-inflation tests (Fig. 1B). Firstly, a flared tip cannula was cautiously inserted into the prepared sIA specimen and secured with a 4.0 silk suture. All minor branches and opposite ends of the analysed arterial segment with sIA were ligated with 7.0 or 4.0 silk sutures, respectively. Next, the sIA was pressurised with a 0.9% NaCl solution at 36°C. In the first stage, the morphometry of the sIA and adjacent cerebral arteries was measured at a constant pressure of 100 mmHg to establish the approximate in vivo dimensions (Fig. 1C).

The diameter of the parent artery was measured 5 mm upstream from the lateral angle. The diameters of both larger and smaller branches were obtained in the same manner, while the diameter of the anterior communicating artery was measured midway between the two anterior cerebral arteries. SIAs were classified as regular when the dome shape approximated a sphere/oval, or as irregular when secondary pouches were identified. Measurements of dimensions and morphometric parameters of the analysed sIAs were obtained as follows (Fig. 2A–D):

- The aneurysm neck diameter (N) was measured at the base of the dome as close as possible to the wall of the parent artery
- Maximal size (Smax) was the largest diameter between the walls of the aneurysm dome, excluding the aneurysm neck, entirely comprised inside the aneurysmal sac
- Orthogonal height (Hortho) was the maximal distance perpendicular to the neck plane between the base and apex of the aneurysm, and orthogonal width (Wortho) was the longest distance parallel to the neck plane
- Maximal height (Hmax) was the longest diameter between the midpoint of the aneurysm neck plane and the most distal point on the aneurysm dome, entirely comprised inside the aneurysmal sac, and maximal width (Wmax) was the largest diameter perpendicular to the Hmax
- Aspect ratio (AR), height/width ratio (HW), and bottleneck factor (BNF) were defined as Hmax/N, Hmax/Wmax, and Wortho/N, respectively [6]
- The size ratio (SR) was calculated by dividing Hmax by the average diameter of the parent artery and both branches [7]; in the case of sIAs localised at the anterior communicating artery, the parent artery was considered as the A1 segment of the anterior cerebral artery, the axis of which was more approximate to Hmax.

Pressure-inflation tests

Our experimental protocol was adapted from our previous study regarding analysis of rupture pressure of cerebral arteries [14]. Five preconditioning cycles were performed with gradually increasing-decreasing pressure ranging from 0 to 200 mmHg, with a speed of 10 mmHg/s for muscle fibre relaxation. Then, the pressure was increased

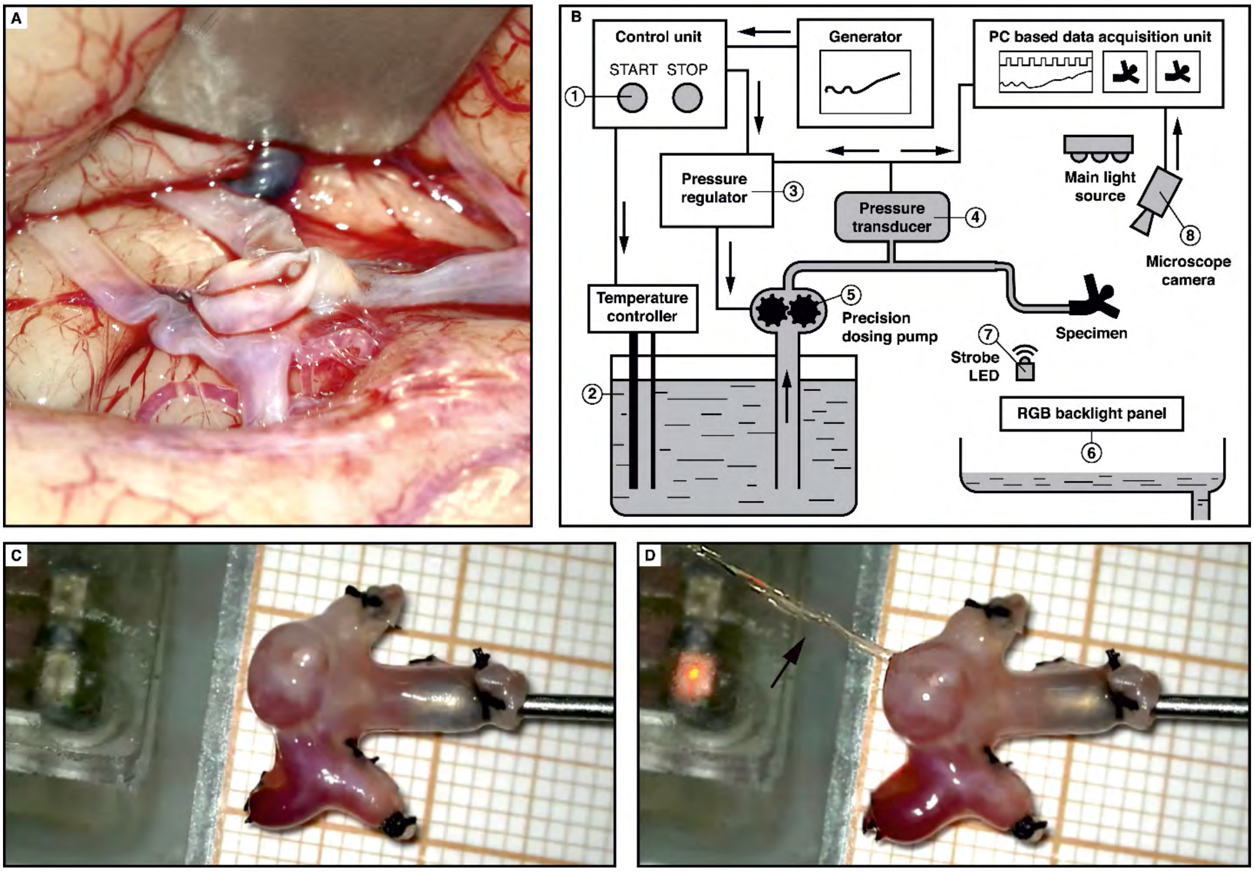

Figure 1. Specimen preparation and pressure-inflation test. **A.** Photograph shows unpressurised left middle cerebral artery bifurcation aneurysm; **B.** Block diagram of working area. Following activation (1), temperature controller regulates temperature of 0.9% NaCl (2) maintaining its predefined value and transmits a specified pressure to pressure regulator (3). Due to feedback signal from pressure transducer (4), regulator maintains proper pressure within analysed aneurysm specimen by controlling precision dosing pump (5). Multicoloured lights (6) provide optimal conditions for visual registration. LED diodes (7) were used to correlate pressure with image from camera (8); **C.** Middle cerebral artery bifurcation aneurysm mounted on flared tip cannula and pressurised to 100 mmHg; **D.** Same aneurysm at moment of rupture; black arrow indicates stream of 0.9% NaCl

continuously at a rate of 20 mmHg/s, which assured quasi-static conditions until the specimen ruptured (Fig. 1D). During the test, increasing pressure values and images of the inflated sIA were registered and stored. The follow-up steering control system regulated the pump revolutions to provide a constant increase in pressure. The rupture site was identified at the end of the experiment. Aneurysms were classified as low WS when the sIA wall ruptured, and as high WS when the rupture occurred within the wall of the adjacent cerebral artery. Differences between sIAs with high and low WS regarding the dimensions, morphometric parameters, and rupture pressure values of the analysed specimens were evaluated.

Statistical analysis

Statistical analyses were performed using the statistical package STATISTICA 13.1 (StatSoft, Inc.) and R environment. All continuous and ordinal variables were summarised as mean and standard deviation (SD). Percentages, numerators, and denominators were presented for categorical and binary variables. Student's t-test for independent samples was used to examine differences between the two groups in continuous variables. Fisher's exact test was used to examine qualitative variables. For all calculations, the statistical significance level was set at $\alpha = 0.05$. P-values were unadjusted for multiple comparisons.

Results

SIAs localisation and morphological data

Table 1 sets out demographic data with the location and morphological characteristics of the analysed sIAs. In three analyzed specimens, the sIA wall ruptured: one anterior communicating artery complex, one internal carotid artery bifurcation, and one middle cerebral artery bifurcation aneurysm. Aneurysms presenting low WS were characterised by

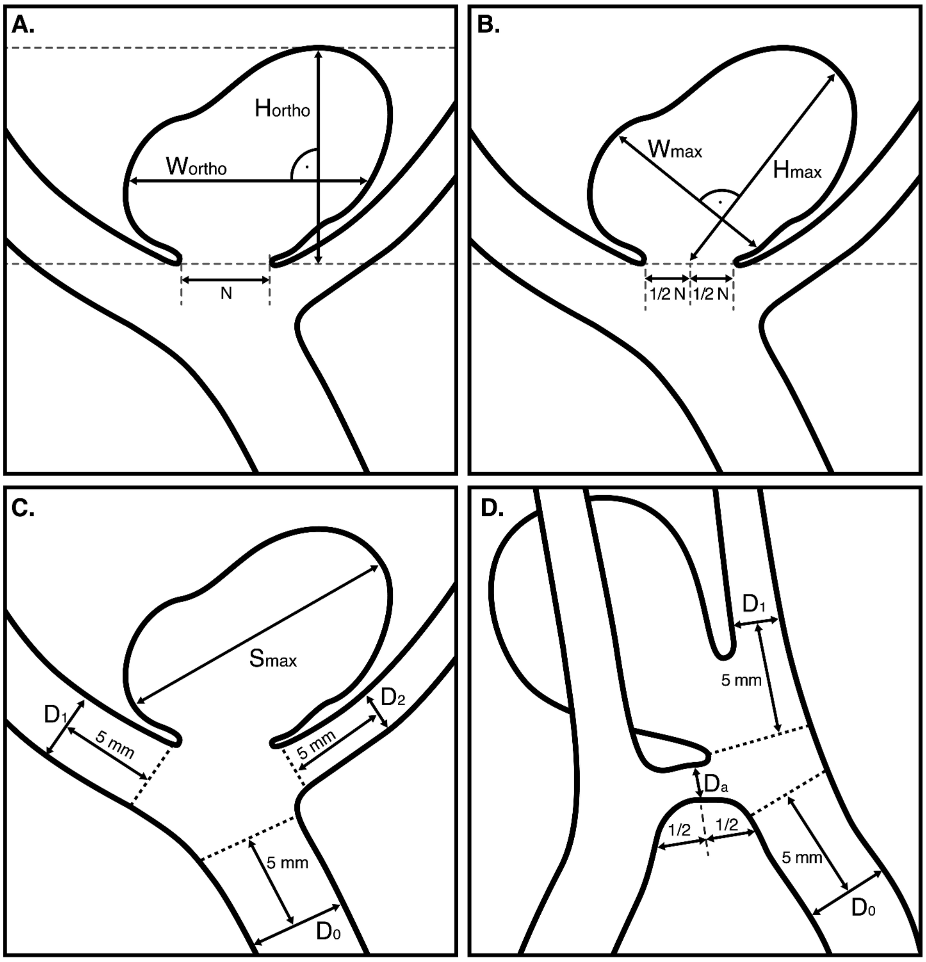

Figure 2. Schematic representation of dimensions of analysed aneurysms measured at intraluminal pressure of 100 mmHg Smax — maximal size; Hmax — maximal height; Hortho — orthogonal height; Wmax — maximal width; Wortho — orthogonal width; N — neck diameter; D0 — parent artery diameter; D1 — larger branch diameter; D2 — smaller branch diameter; Da – anterior communicating artery diameter. For detailed description of measurement methodology, see 'Materials and methods' above

significantly increased Smax ($p = 0.034$), Hortho ($p = 0.005$), Wmax ($p = 0.002$), and Wortho ($p = 0.030$) compared to sIAs that did not rupture during the experiments. No differences among values of AR, SR, HW, and BNF between sIAs with low and high WS were observed (Tab. 2). Irregular dome shape was observed in 2/3 (66.7%) and in 1/5 (20%) of cases in the group of sIAs that ruptured and did not rupture respectively during pressure-inflation tests. No significant difference between the two WS categories in terms of irregular dome shape was observed.

Rupture pressure values

The mean sIA rupture pressure was 769 ± 230 mmHg (range: 596–1,030 mmHg). In cases where the rupture occurred at the arterial wall, the average rupture pressure was 1,259 ± 256 mmHg (range: 813–1,462 mmHg). Significantly lower value of mean rupture pressure of the sIA wall compared to the arterial wall was observed ($p = 0.035$).

Discussion

Wall strength in relation to natural history of unruptured sIAs

In the present study, dome dimensions, except for Hmax, were significantly increased among sIAs with low WS compared to sIAs with high WS. Prospective observational studies of unruptured sIAs have revealed that dome size is strongly related to the annual rupture rate of sIAs. According to the multicentre UCAS Japan study, sIAs with dome sizes of 3–4 mm are characterised by an extremely low rupture risk which increases considerably in cases of sIAs ≥ 7 mm [2]. Furthermore, in a lifelong Finnish observational study, nearly 80% of ruptured sIAs that were small at the beginning increased their dome size to ≥ 7 mm by the time of SAH [10]. However, the threshold size for rupture prediction is still uncertain. This may result from the fact that different dome dimensions

Table 1. Demographic data and intracranial aneurysm characteristics

Age	Sex	Cause of death	Aneurysm location	Rupture pressure [mmHg]	Rupture site	Irregular shape	Smax [mm]	Hmax [mm]	Hortho [mm]	Wmax [mm]	Wortho [mm]	N [mm]	AR	SR	HW	BNF
60	M	Acute myocardial infarction	RMCA bif	1,321	Artery	+	2.89	2.04	1.87	2.43	2.74	2.26	0.90	0.67	0.84	1.21
60	M	Suicidal hanging	LMCA bif	1,462	Artery	–	1.84	1.10	1.04	1.87	1.83	2.03	0.54	0.35	0.59	0.90
63	F	Generalised cancer	LICA bif	1,309	Artery	–	2.39	1.70	1.50	2.21	2.28	2.05	0.83	0.47	0.77	1.11
69	M	Alcohol poisoning	ACommA	813	Artery	–	2.72	2.22	2.12	2.80	2.57	2.33	0.95	0.68	0.79	1,10
61	M	Alcohol poisoning	LICA bif	1,388	Artery	–	2.31	1.23	0.96	2.3	2.17	2.70	0.46	0.33	0.53	0.80
55	F	Pneumonia	ACommA	681	Aneurysm	+	10.34	8.51	2.92	5.85	10.18	2.82	3.02	3.86	1.45	3.61
67	M	Suicidal hanging	LMCA bif	596	Aneurysm	–	5.32	3.21	3.11	5.11	5.23	4.35	0.74	1.11	0.63	1.20
58	M	Drowning	LICA bif	1,030	Aneurysm	+	3.73	2.62	2.59	3.73	3.72	2.20	1.19	0.70	0.70	1.69

+ — present; – — absent; ACommA — anterior communicating artery; AR — aspect ratio; BNF — bottleneck factor; F — female; Hmax — maximum height; Hortho — orthogonal height; HW — height/width ratio; ICA bif — internal carotid artery bifurcation; L — left; M — male; MCA bif — middle cerebral artery bifurcation; N — neck diameter; R — right; Smax — maximal size; SR — size ratio; Wmax — maximal width; Wortho — orthogonal width

determining the size of sIAs were used in various studies [7, 9]. Based on the study by Lauric et al., the sIAs threshold size for rupture status assessment was calculated at 7.33 mm, 7.71 mm, and 5.43 mm for Smax, Wortho, and Hortho, respectively [6]. In our study, dome dimensions of two pressurised sIAs that ruptured during the experiments were smaller than the referenced threshold values. However, although the sIA rupture pressure was significantly lower than the rupture pressure of the analysed cerebral arteries, the obtained rupture pressures of the sIAs still markedly exceeded the maximum values of in vivo arterial blood pressure [15]. This is consistent with the results of an earlier report concerning rupture pressure values of unruptured sIAs. In the study by Scott et al., sIAs with dome sizes of 5 mm and 6 mm extracted from human subjects during post mortems were pressurised with saline solution. The smaller sIA ruptured at 325 mmHg, but the second one was stable after eight repeated pressure loadings to 550 mmHg [16]. It may be hypothesised that none of the analysed sIAs could rupture under physiological conditions at the time of our study. Nevertheless, based on clinical practice and retrospective analyses, a significant percentage of ruptured sIAs are < 5 mm [4, 5]. Despite the fact that the rupture of a small sIA may occur soon after formation [17], small sIAs representing slow growth patterns may also be the cause of SAH. In another multicentre SUAVe study that included only unruptured sIAs < 5 mm, among 448 sIAs, seven ruptured and 30 increased in size during the follow-up period, and a dome diameter ≥ 4 mm was identified as a risk factor for both rupture and growth of small sIAs [3].

Our study revealed that all of the sIAs that ruptured during pressure-inflation tests were > 3 mm. In contrast, in all sIAs that sustained even supraphysiological pressure loadings, the dome dimensions measured < 3 mm, confirming that such small sIAs may be at an extremely low risk of rupture [3].

Morphological rupture risk factors

Haemodynamic conditions in the lumen of the sIA also affect the risk of rupture and are related not only to sIA dimensions, but also to the shape of its dome. It has been shown that bloodflow within the lumen of ruptured sIAs is characterised by complex and unstable flow vortices in the regions of flow stagnation and low wall shear stress [18]. A similar complexity of flow patterns eliciting low wall shear stress zones has been observed in sIAs with higher values of dome morphometric parameters [19].

This flow-related association of morphometric parameters with the risk of sIA rupture is in line with the results of the study by Kleinloog et al. Their systematic review and meta-analysis revealed that irregular dome shape and sIA morphometric parameters such as AR, HW, BNF and SR are strongly associated with increased rupture risk [20]. In our study, none of these morphometric parameters significantly differed between sIAs with low and high WS. The clear discrepancies between our results and the literature data regarding

Table 2. Morphological data of saccular intracranial aneurysms regarding aneurysm wall strength

	Aneurysm wall strength*				
	Low		High		
	mean	SD	mean	SD	P-value
Aspect ratio (AR)	1.65	1.21	0.74	0.22	0.134
Size ratio (SR)	1.89	1.72	0.50	0.17	0.106
Height/width ratio (HW)	0.93	0.46	0.71	0.13	0.326
Bottleneck factor (BNF)	2.17	1.27	1.03	0.17	0.082
Maximal size (Smax) [mm]	6.46	3.45	2.43	0.41	0.034
Maximal height (Hmax) [mm]	4.78	3.24	1.66	0.49	0.067
Orthogonal height (Hortho) [mm]	2.87	0.26	1.50	0.51	0.005
Maximal width (Wmax) [mm]	4.90	1.08	2.32	0.34	0.002
Orthogonal width (Wortho) [mm]	6.38	3.38	2.32	0.35	0.030
Neck diameter (N) [mm]	3.12	1.11	2.27	0.27	0.136

*Low wall strength corresponds to aneurysms that ruptured during pressure-inflation tests; high wall strength reflects aneurysms that sustained pressurisation. SD — standard deviation

morphometric parameters related to an increased rupture risk may result from the fact that most of these parameters are derived from cross-sectional studies comparing the morphology of ruptured and unruptured sIAs. Additionally, there is increasing evidence that sIAs tend to change their geometry after rupture. Skodvin et al. retrospectively analysed pre- and post-rupture radiological data of 29 sIAs, with a median period of 12 months between the two imaging studies. All dome diameters were significantly larger, and the degree of the size increment was positively corelated with the time elapsed between pre- and post-rupture radiological images [8]. The same Norwegian research team conducted another radiological study addressing morphometric parameters, but this time of only unruptured sIAs. The authors compared the morphological characteristics of sIAs that later ruptured to a control group of sIAs that remained stable during the follow-up and that were matched in terms of age, sex, sIA size, and location. Consistent with our results, none of the aforementioned morphometric parameters were associated with subsequent rupture [9].

Thus, we suggest that AR, HW, BNF, and SR are inadequate for rupture risk assessment of currently unruptured sIAs.

Limitations

There were some limitations of our study. Due to the small number of specimens, it was not possible to categorise sIAs into low and high WS categories in specific locations. Also, considering the small dimensions of the analysed sIAs, it was not possible to pressurise isolated sIAs. Hence, rupture pressure was obtained only in three sIAs and was compared to rupture pressure of cerebral arteries.

For this reason, the obtained values of rupture pressure overlapped between both analysed groups, and the actual values of sIAs with high WS are still unknown. Furthermore, the conditions during pressure-inflation tests do not represent in vivo conditions. Firstly, to provide reproducible pressure loadings, the pressures within the isolated specimens were increased quasi-statically, simultaneously neglecting haemodynamic factors that are important during pathogenesis of the sIAs [18, 19]. Secondly, both cerebral arteries and sIAs are normally surrounded by cerebrospinal fluid, which imposes a pressure on the arterial wall greater than atmospheric pressure. Since our experiments were conducted outside the cranial cavity, our results may not completely reflect the in vivo rupture pressure values of the analysed sIAs. Next, our experiments were conducted on sIA specimens collected from post mortem subjects within 36 hours of death. Thus, the autolysis process could have affected the analysis of the rupture pressure of the sIA wall. Nevertheless, only those studies concerning biomechanical analysis of sIA specimens collected post mortem allow for the assessment of aneurysm WS in relation to the WS of adjacent cerebral arteries.

Finally, our study did not consider microstructural degenerative changes within the wall of the sIAs. According to the literature data, the walls of ruptured and unruptured sIAs differ in terms of matrix remodelling, decellularisation and inflammatory cell infiltration [21, 22]. Further studies concerning biomechanical experiments with additional analysis of sIA walls on a histological level may help to identify which unruptured small sIAs are prone to rupture.

Conclusions

In our study, none of the analyzed sIAs ruptured at physiological pressure values. Furthermore, sIAs with domes < 3 mm sustained pressure values causing rupture of the neighbouring parent artery or its branches, while sIAs with domes measuring > 3 mm were characterised by lower WS than the strength of the adjacent cerebral arteries. Morphometric parameters such as AR, SR, HW, and BNF and irregular dome shape were not associated with the WS of the analyzed sIAs. Thus, dome dimension was the only distinctive feature categorising sIAs into low or high WS.

Clinical implications/future directions

Our results support observations that the rupture risk of sIAs increases with increasing dome size, and that unruptured sIAs with domes < 7 mm are at low risk of rupture. Moreover, in such small sIAs, dome diameter may be more useful than other morphometric parameters such as AR, SR, HW, and BNF for assessing the risk of rupture. Since all of the analysed sIA specimens were < 7 mm in size, and ruptured or would rupture under supraphysiological pressure loadings, further studies are needed with larger sample sizes considering the morphology and biomechanical properties of unruptured sIAs to better elucidate which sIAs are at greater risk of rupture, and thus which should be treated invasively.

Conflicts of interest: *None.*
Funding: *None.*

References

1. Kang H, Peng T, Qian Z, et al. Impact of hypertension and smoking on the rupture of intracranial aneurysms and their joint effect. Neurol Neurochir Pol. 2015; 49(2): 121–125, doi: 10.1016/j.pjnns.2015.03.005, indexed in Pubmed: 25890927.
2. Morita A, Kirino T, Hashi K, et al. UCAS Japan Investigators. The natural course of unruptured cerebral aneurysms in a Japanese cohort. N Engl J Med. 2012; 366(26): 2474–2482, doi: 10.1056/NEJMoa1113260, indexed in Pubmed: 22738097.
3. Sonobe M, Yamazaki T, Yonekura M, et al. Small unruptured intracranial aneurysm verification study: SUAVe study, Japan. Stroke. 2010; 41(9): 1969–1977, doi: 10.1161/STROKEAHA.110.585059, indexed in Pubmed: 20671254.
4. Forget TR, Benitez R, Veznedaroglu E, et al. A review of size and location of ruptured intracranial aneurysms. Neurosurgery. 2001; 49(6): 1322–1355; discussion 1325-1326, doi: 10.1097/00006123-200112000-00006, indexed in Pubmed: 11846931.
5. Lee GJ, Eom KS, Lee C, et al. Rupture of very small intracranial aneurysms: incidence and clinical characteristics. J Cerebrovasc Endovasc Neurosurg. 2015; 17(3): 217–222, doi: 10.7461/jcen.2015.17.3.217, indexed in Pubmed: 26526401.
6. Lauric A, Baharoglu MI, Malek AM. Ruptured status discrimination performance of aspect ratio, height/width, and bottleneck factor is highly dependent on aneurysm sizing methodology. Neurosurgery. 2012; 71(1): 38–45, doi: 10.1227/NEU.0b013e3182503bf9, indexed in Pubmed: 22353797.
7. Dhar S, Tremmel M, Mocco J, et al. Morphology parameters for intracranial aneurysm rupture risk assessment. Neurosurgery. 2008; 63(2): 185–96; discussion 196, doi: 10.1227/01.NEU.0000316847.64140.81, indexed in Pubmed: 18797347.
8. Skodvin TØ, Johnsen LH, Gjertsen Ø, et al. Cerebral aneurysm morphology before and after rupture: nationwide case series of 29 aneurysms. Stroke. 2017; 48(4): 880–886, doi: 10.1161/STROKEAHA.116.015288, indexed in Pubmed: 28265012.
9. Skodvin TØ, Evju Ø, Sorteberg A, et al. Prerupture intracranial aneurysm morphology in predicting risk of rupture: a matched case-control study. Neurosurgery. 2019; 84(1): 132–140, doi: 10.1093/neuros/nyy010, indexed in Pubmed: 29529238.
10. Korja M, Lehto H, Juvela S, et al. Lifelong rupture risk of intracranial aneurysms depends on risk factors: a prospective Finnish cohort study. Stroke. 2014; 45(7): 1958–1963, doi: 10.1161/STROKEAHA.114.005318, indexed in Pubmed: 24851875.
11. Darsaut TE, Keough MB, Boisseau W, et al. CURES Collaborative Group. The design of the canadian unruptured endovascular versus surgery (CURES) trial. Can J Neurol Sci. 2011; 38(2): 236–241, doi: 10.1017/s0317167100011392, indexed in Pubmed: 21320826.
12. Costalat V, Sanchez M, Ambard D, et al. Biomechanical wall properties of human intracranial aneurysms resected following surgical clipping (IRRAs Project). J Biomech. 2011; 44(15): 2685–2691, doi: 10.1016/j.jbiomech.2011.07.026, indexed in Pubmed: 21924427.
13. Robertson AM, Duan X, Aziz KM, et al. Diversity in the strength and structure of unruptured cerebral aneurysms. Ann Biomed Eng. 2015; 43(7): 1502–1515, doi: 10.1007/s10439-015-1252-4, indexed in Pubmed: 25632891.
14. Piechna A, Lombarski L, Krajewski P, et al. Age dependence of critical pressure in the segments and branches of the circle of Willis. Neurol Neurochir Pol. 2017; 51(2): 146–148, doi: 10.1016/j.pjnns.2017.01.003, indexed in Pubmed: 28187986.
15. MacDougall JD, Tuxen D, Sale DG, et al. Arterial blood pressure response to heavy resistance exercise. J Appl Physiol (1985). 1985; 58(3): 785–790, doi: 10.1152/jappl.1985.58.3.785, indexed in Pubmed: 3980383.
16. Scott S, Ferguson GG, Roach MR. Comparison of the elastic properties of human intracranial arteries and aneurysms. Can J Physiol Pharmacol. 1972; 50(4): 328–332, doi: 10.1139/y72-049, indexed in Pubmed: 5038350.
17. Mitchell P, Jakubowski J. Estimate of the maximum time interval between formation of cerebral aneurysm and rupture. J Neurol Neurosurg Psychiatry. 2000; 69(6): 760–767, doi: 10.1136/jnnp.69.6.760, indexed in Pubmed: 11080228.
18. Cebral JR, Mut F, Weir J, et al. Association of hemodynamic characteristics and cerebral aneurysm rupture. AJNR Am J Neuroradiol. 2011; 32(2): 264–270, doi: 10.3174/ajnr.A2274, indexed in Pubmed: 21051508.
19. Tremmel M, Dhar S, Levy EI, et al. Influence of intracranial aneurysm-to-parent vessel size ratio on hemodynamics and implication for rupture: results from a virtual experimental study. Neurosurgery. 2009; 64(4): 622–630; discussion 630–631, doi: 10.1227/01.NEU.0000341529.11231.69, indexed in Pubmed: 19349824.
20. Kleinloog R, de Mul N, Verweij BH, et al. Risk factors for intracranial aneurysm rupture: a systematic review. Neurosurgery. 2018; 82(4): 431–440, doi: 10.1093/neuros/nyx238, indexed in Pubmed: 28498930.
21. Frösen J, Piippo A, Paetau A, et al. Remodeling of saccular cerebral artery aneurysm wall is associated with rupture: histological analysis of 24 unruptured and 42 ruptured cases. Stroke. 2004; 35(10): 2287–2293, doi: 10.1161/01.STR.0000140636.30204.da, indexed in Pubmed: 15322297.
22. Kataoka K, Taneda M, Asai T, et al. Structural fragility and inflammatory response of ruptured cerebral aneurysms. A comparative study between ruptured and unruptured cerebral aneurysms. Stroke. 1999; 30(7): 1396–1401, doi: 10.1161/01.str.30.7.1396, indexed in Pubmed: 10390313.